CHAPTER 140

PROFILE CHANGE OF A SHEET FLOW DOMINATED BEACH

Mohammad Dibajnia [1], Takuzo Shimizu [2] and Akira Watanabe [3]

Abstract

A new and detailed model for predicting the profile change of a real beach is presented. The model is based on the sediment transport formula of Dibajnia and Watanabe (1992) and therefore incorporates, explicitly, the asymmetry of the near-bottom orbital velocity and the undertow into the transport of bottom sediment. Its applicability is examined by using the data of beach profile change obtained from prototype scale laboratory experiments as well as field measurements. It is shown that quite accurate profile simulation is possible when the details of the flow field and transport mechanism are considered.

1. Introduction

An important phenomenon concerned in short-term prediction of nearshore bottom topography changes is the formation and disappearance of longshore bar systems. It is now clear that during storms, usually the shoreward sheet flow sediment transport due to large waves faces the seaward transport of the undertow in a region close to the breaking point and makes a bar. This bar in turn, may be washed out by the undertow of some larger waves and move to deeper waters, or it could be forced by the shoreward transport of other waves to move into shallower waters and form a smaller bar or recover the beach. Also we know that under field conditions, sheet flow movement is the predominant transport mode

[1]Associate Professor, Dept. of Civil Eng., Univ. of Tokyo, Bunkyo-ku, Tokyo 113, Japan.
[2]Penta-Ocean Construction Co. Ltd., 2-2-8 Koraku, Bunkyo-ku, Tokyo 112, Japan.
[3]Professor, Dept. of Civil Eng., Univ. of Tokyo, Bunkyo-ku, Tokyo 113, Japan.

over a significant part of the nearshore area including both inside and outside of the surf zone.

In the present study a numerical model for simulating the profile transformation of a real beach is presented. The model is based on sediment transport formula of Dibajnia and Watanabe (1992) which incorporates the asymmetry of near bottom orbital velocity and superimposed currents into estimating the sheet flow sand transport rates. The formula is extended here to cover suspended load as well as bed load transports. Applicability of the model is confirmed through comparison of the simulated profiles with those obtained from prototype scale laboratory experiments and field data. A new formulation for estimating the return flow velocity in the field is also presented.

2. Experimental and Field Data

Kajima *et al.* (1982) investigated on-offshore beach profile changes under regular waves in a prototype scale wave flume for a variety of incident wave, bottom slope, and grain size conditions. Two of their experimental cases, corresponding to extreme conditions of erosion and accretion, are selected to be tried against the present model. The conditions for each case are shown in Table 1. In this table $\tan\beta$ is the initial bottom slope, d_{50} the median grain size of beach meterial, T the wave period, and H_0 the deepwater wave height.

CASE	$\tan\beta$	d_{50} mm	T s	H_0 m	Breaker form
3-3	5/100	0.27	12.0	0.65	plunging
3-4	5/100	0.27	3.1	1.62	spilling

Table 1: Experimental conditions

The field measurement data are those reported by Kuriyama (1991) and have been obtained at Hazaki Oceanographical Research Facility (HORF) which belongs to the Port and Harbour Research Institute of the Japanese Ministry of transport and is located at Kashima beach, Ibaraki Prefecture, Japan. The average bottom slope at the site is about 1/60 and the median grain size, d_{50}, is 0.18 mm. The field investigations have been conducted from the 12th to 26th of September 1988, during which a strong storm has occurred. Profile survey data at the begining and end of this period are given. Time histories of the offshore significant waves at a mean depth of about 24 m and those of wave height, bottom elavation, tidal level, and cross-shore steady current at a point inside the surf zone, P145, are also reported. The graphical data are transfered to digital data with an interval of two hours by using a digitizer and are used and demonstrated in the present paper.

3. Elements of The Model

3.1 Calculation of the wave field

For regular waves, the time-dependent mild-slope equations and numerical scheme of Watanabe and Dibajnia (1988) are used. The equations can take care of wave shoaling, reflection, breaking, and energy dissipation in cross-shore direction. Location of the breaking point is calculated with the generalized breaker index diagram proposed by Watanabe *et al.* (1984).

As for the calculation of the waves in the field, the method proposed by Isobe (1987) for irreguler waves is applied. This model is based on an energy conservation equation which contains a breaking dissipation term. The equation which can take care of wave shoaling, breaking, and energy dissipation in cross-shore direction reads:

$$\frac{d}{dx}(Ec_g) = -\frac{5}{2}P_B E\sqrt{\frac{g}{h}}\sqrt{\frac{\alpha_{1/3}-\alpha_r}{\alpha_s-\alpha_r}}f_d(kh)\tan\beta \tag{1}$$

in which E is the total wave energy, x the cross-shore distance, g the acceleration of gravity, α the ratio of water particle velocity at the wave crest to the wave celerity, c_g the group velocity, f_d a function of the wave number k and the water depth h given by Isobe (1987), and $\tan\beta$ the local bottom slope. Values of c_g and f_d should be calculated by using the peak frequency of the spectrum. $\alpha_r = 0.135$ and $\alpha_s = 0.4(0.57 + 5.3\tan\beta)$ are the values of α for broken waves recovered in a uniform depth region and for breaking waves on a uniform slope, respectively (see Dibajnia and Watanabe, 1988). In the above equation P_B is the breaking probability and is obtained from the following relation

$$P_B = \left\{1 + 2.004\left(\frac{\alpha_b}{\alpha'_{1/3}}\right)^2\right\}\exp\left[-2.004\left(\frac{\alpha_b}{\alpha'_{1/3}}\right)^2\right] \tag{2}$$

where α_b is the critical value of α for breaking and $\alpha'_{1/3}$ is the value of α if the waves continue to shoal without breaking. By using P_B, Equation (1) can be used for both outside and inside of the surf zone.

For both regular and irregular waves, the change in the position of shoreline due to the setup of mean water level (and tides) is incorporated through applying a moving boundary technique which allows a variable grid size at the shoreline.

3.2 Estimation of the near-bottom velocity profile

In reality, waves are nonlinear due to finite depth and asymmetric due to the bottom slope. Despite recent developements in applying Boussinesq equations to predicting the relevant properties of waves over the whole nearshore region, an empirical method is applied in the present study to estimate the near-bottom

velocity profiles. This is because that only information about significant wave height and period of the incident waves are available for the field case. Isobe and Horikawa (1981), based on laboratory experiments, proposed empirical formulas for estimation of velocity profile properties of normally incident waves on a beach with uniform slope up to the point of breaking. The validity of their relations for estimation of velocity profile of prototype-scale shoaling waves over an erodible bed has been verified by Maruyama *et al.* (1983). In the absence of a reliable theory or formulation for breaking waves, in the present work the method of Isobe and Horikawa (1981) is applied to the surf zone region as well as the offshore region. It has been shown in a separate paper (Dibajnia *et al.*, 1992) that inside the surf zone, the method of Isobe and Horikawa gives reasonable results for spilling breakers, but fails to predict the velocity profile of plunging breakers accurately.

The method is also applied to estimating the asymmetry of orbital velocity profile at the bottom for irregular waves by using values of the significant wave height and period. According to the experimental study of Sato *et al.* (1988), the asymmetry of velocity profile in the surf zone is less than those in the offshore and in the breaking region. Therefore, the estimated velocity profiles inside the surf zone are modified gradually from the breaking point to the shoreline.

3.3 Calculation of the undertow

Undertow is the name given to the average seaward return flow found below wave trough level. It balances the mass flux curried shoreward by breaking waves including the effect of the surface roller. Despite its simple qualitative description, a general mathematical formulation of the undertow and its vertical distribution is difficullt and not yet available. For regular waves over simple bottom profiles, Okayasu *et al.* (1990) took the mass balance approach and presented a model based on the experimental results and the assumption that following the breaking, the wave energy is transferred to the roller or large vortices, is kept by them for a while, then is conveyed to the small structure turbulence and is dissipated. The time-dependent mild-slope equations of Watanabe and Dibajnia (1988) were used to estimate the rate of energy transfer. The model showed good agreement with the experiments, however, its application to more general cases is not straightforward.

A simple model based on the assumption that the mass flux of a bore propagating shoreward is proportional to the square of the wave height was presented by Sato *et al.* (1988). By assuming that the corresponding return flow is uniform over the local mean water depth, D, the steady component of near-bottom velocity was estimated as

$$U = U_w + U_b + U_e \tag{3}$$

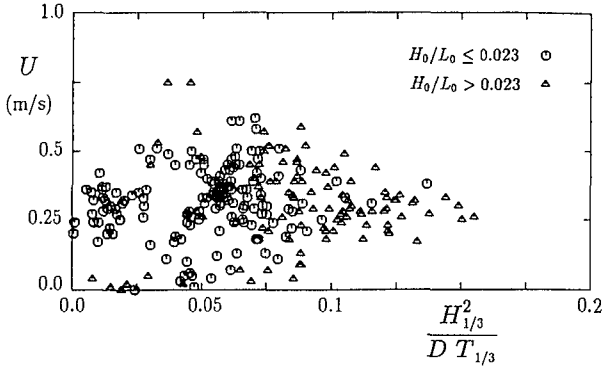

Figure 1: **Undertow velocity measured at the point P145 versus Eq. (4).**

in which U_b is the undertow velocity given as

$$U_b = -A\frac{H^2}{D \cdot T} \tag{4}$$

, U_w the offshore flow compensating the onshore mass flux due to the irrotational wave motion, U_e the Eulerian mass transport velocity at the edge of the laminar boundary layer, T the wave period, H the wave height, and A a nondimensional coefficient of the order of unity. These two models are used here for calculating the undertow velocity of regular waves.

For the irregular waves in the field, in order to examine the applicability of Eq. (4) to estimating the undertow velocity caused by breaking, values of the significant wave height, $H_{1/3}$, and the mean water depth measured at the point P145, together with the values of the significant wave period, $T_{1/3}$, of offshore waves are substituted into Equation (4) and the results are compared with the measured values of the cross-shore mean current velocity at P145 as shown in Fig. 1. A large scatter is observed and it is hard to define a value for the coefficient A. Those data with a deepwater wave steepness greater than 0.023 are shown by triangle symbols. It may be seen that these data are more or less separated from the others. On the other hand, it is expected that the undertow velocity varies with the beach slope. From these two points one may conclude that the undertow velocity should depends on the surf similarity parameter, $\xi = \tan\beta/\sqrt{H_0/L_0}$, which is often used to classify the breaker types. Thus, the return flow velocity should vary with the breaker type, as it is indeed a breaking generated process. Also, using the bottom slope at the breaking point, $(\tan\beta)_b$, would be more appropriate than $\tan\beta$. Figure 2 shows the results of such an analysis when $\xi_b = (\tan\beta)_b/\sqrt{H_0/L_0}$ is used instead of ξ. In this figure it is assummed, considering the incident waves, that during the first half of the measurement period the waves were breaking in deeper waters on a slope of 1/60 because they were large (see Fig. 8), and during the second half they were breaking on the bar closer to the

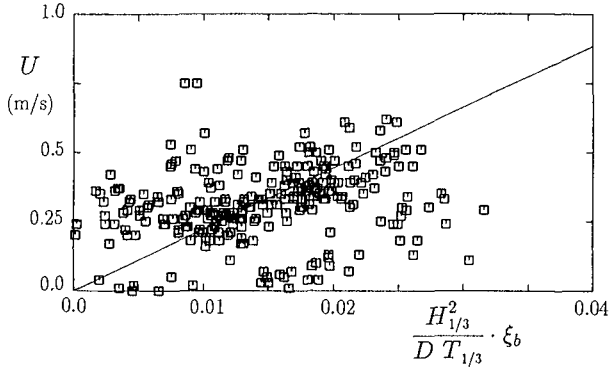

Figure 2: **Undertow velocity measured at the point P145 versus Eq. (5).**

shore with a slope of about 1/25. It can be seen that the data show a good trend which may be written as

$$U_b = -22 \frac{H_{1/3}^2}{D \cdot T_{1/3}} \cdot \xi_b \tag{5}$$

The next problem regarding the undertow of irregular waves is about its distribution in cross-shore direction. In case of regular waves there is a certain breaking point which controls the distribution. For irregular waves, however, there is not such a point and at any location some of the waves may break because waves of different heights and periods are envolved. At each point it is only this breaking portion of the waves which contributes to the generation of the undertow. Thus, considering the ratio of the energy of the broken waves to the total wave energy we may write

$$U = -22 \left(1 - \frac{E}{E'}\right) \frac{H_{1/3}^2}{D \cdot T_{1/3}} \cdot \xi_b \tag{6}$$

for irregular waves. Here, E is the total wave energy, and E' the total wave energy of an imaginary case in which the same waves shoal without breaking. P145 is a point inside the surf zone where all the waves are expected to break and hence $E/E' \simeq 0$. At other locations, however, because of irregularity only part of the waves may break and it is only this breaking portion of the waves which is taken into account.

3.4 Sediment transport rate

The sediment transport formula of Dibajnia and Watanabe (1992) is used. This formula has been made for the transport under sheet flow conditions, but is extended here to be able of estimating the suspended load and bed load transport

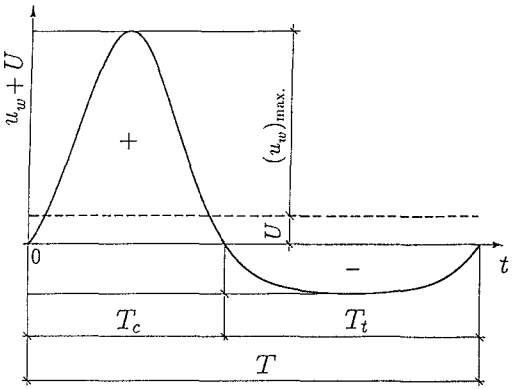

Figure 3: **Definitions for the near-bottom velocity profile.**

rates as well. The nondimensional net transport rate, Φ_s, is obtained by

$$|\Phi_s| = \frac{q_s(1-\epsilon)}{Wd} = 0.001 \cdot \text{sign}(\Gamma) \cdot |\Gamma|^{0.55} \tag{7}$$

where

$$\Gamma = \frac{u_c T_c(\Omega_c^3 + \Omega_t'^3) - u_t T_t(\Omega_t^3 + \Omega_c'^3)}{(u_c + u_t)T} \tag{8}$$

in which u_c and u_t are the equivalent sinusoidal velocity amplitudes of positive and negative portions of the near-bottom velocity profile including the steady current (Fig. 3), respectively, and are defined as

$$u_c^2 = \frac{2}{T_c}\int_0^{T_c}(u_w + U)^2 dt \quad \text{and} \quad u_t^2 = \frac{2}{T_t}\int_{T_c}^{T}(u_w + U)^2 dt \tag{9}$$

with T_c and T_t being their corresponding time durations, respectively, and u_w the near-bottom orbital velocity. Values of Ω_j in Eq. (8) are obtained as follows.

$$\begin{cases} \text{if } \omega_j \le \omega_{\text{critical}} & \begin{cases} \Omega_j = \omega_j \cdot \dfrac{2WT_j}{d} \\ \Omega_j' = 0 \end{cases} \\ \text{if } \omega_j > \omega_{\text{critical}} & \begin{cases} \Omega_j = \omega_{\text{critical}} \cdot \dfrac{2WT_j}{d} \\ \Omega_j' = (\omega_j - \omega_{\text{critical}}) \cdot \dfrac{2WT_j}{d} \end{cases} \end{cases} \tag{10}$$

with

$$\omega_j = \frac{1}{2}\frac{u_j^2}{sgWT_j} \tag{11}$$

In the above relations q_{net} is the net volumetric transport rate, ϵ the sediment porosity, d the sediment grain size, W the sediment fall velocity, $s = (\rho_s - \rho)/\rho$ where ρ and ρ_s are the densities of water and sediment, respectively, and the

subscript j should be replaced by either c or t. It should be mentioned that the factor 2 in relations (10) has been mistakenly omitted in the original paper of Dibajnia and Watanabe (1992).

In order to extend this formulation to estimate suspended load and bed load transport rates, we note that in the actual phenomenon at the sea bottom there is a transition region between the rippled bottom of suspended load and the flat bed of sheet flow. Over this region, the ripple height decreases, and the net transport rate changes its direction from the seaward suspended load to the shoreward sheet flow. Furthermore, experimental results show that $\omega_{\text{critical}} = 1$ for sheet flow transport (Dibajnia and Watanabe, 1992), while $\omega_{\text{critical}} = 0.03$ for the transport over ripples (Suzuki *et. al*, 1994). Therefore, by gradually changing the critical value of ω from unity to a value of 0.03, an effect similar to the above phenomenon can be simulated. Thus

$$\omega_{\text{critical}} = 1 - 0.97\sqrt{\Lambda} \tag{12}$$

in which the parameter Λ is given by

$$\Lambda = \left[1 - [(\Psi_{\text{rms}} - 0.2)/0.4]^2\right] \cdot \min(1, 2\lambda/d_0) \tag{13}$$

where Ψ_{rms} is the Shields number estimated in terms of the root mean square of near bottom velocity profile, λ the ripple wavelength, and d_0 the orbital diameter of water particle displacement at the bottom. In this relation it is assumed that the transition from rippled bed to flat bed occurs in a parabolic manner as the Shields number increases from 0.2 to 0.6. For $\Psi_{\text{rms}} > 0.6$, which corresponds to the sheet flow condition, Λ should be set equal to zero. When $\Psi_{\text{rms}} < 0.2$ then $\Lambda = 1.0$. The last term takes care of the fact that when d_0 is much larger than λ on a rippled bed, the net transport rate should be in onshore direction. The functional form of Eq. (13), however, needs further varification. Also, the limiting values of the Shields number in this equation should be modified if Eq. (7) is to be tried against laboratory data on net sediment transport rate.

4. Results and Discussion

4.1 Prototype scale laboratory experiments

Profile change simulation of each experimental case is conducted for 15 hours of wave action and with both of the undertow models of Okayasu *et al.* (1990) and Sato *et al.* (1988), Eq. (3). Longer time durations are not tried because of the decrease in the accuracy of these models over complicated topographies. It is assumed that the undertow velocity is uniform over the local depth. In both of the models, the calculated steady currents are multiplied by hyperbolic functions in a region from the transition point to a point which is ten times of the breaking depth far from the breaking point in the offshore direction, so as to assume values of zero in the offshore region. The position of transition point is estimated by the

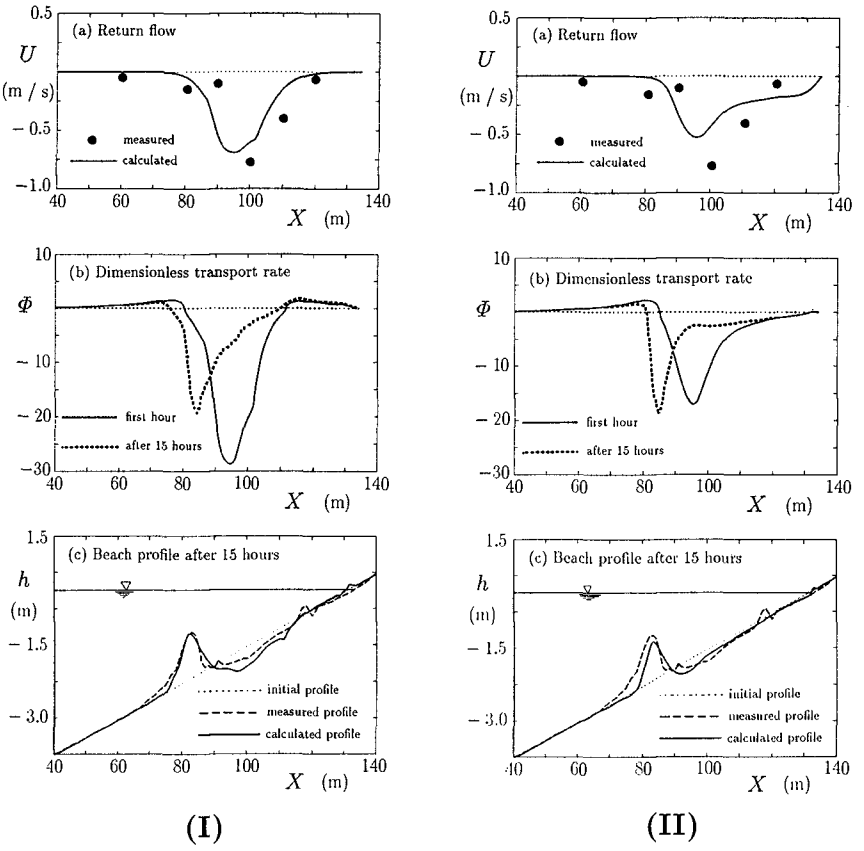

Figure 4: **Simulation results for Case 3-4 with the undertow model of (I) Sato *et al.* and (II) Okayasu *et al.*.**

formula of Okayasu *et al.* (1990). Steady current velocities obtained by the model of Sato *et al.* are multiplied by a hyperbolic function also in the region between the transition point and shoreline in order to obtain a more realistic distribution.

Figures 4 and 5 show the numerical simulation results and their comparison with the measurements. It is observed that the return flow calculated by Sato *et al.*'s model (with $A = 4$) agree well with the experimental data for case 3-4. It should be noticed that this case has a breaker of spilling form. Therefore, the method of Isobe and Horikawa for calculation of near-bottom velocity profile is supposed to give reasonable profiles. As a result it is seen that the development of bottom profile and the position of bar are fairly well simulated. When the model of Okayasu *et al.* is applied to this case, also reasonable results are obtained.

On the other hand, the model of Sato *et al.* considerably underestimates the

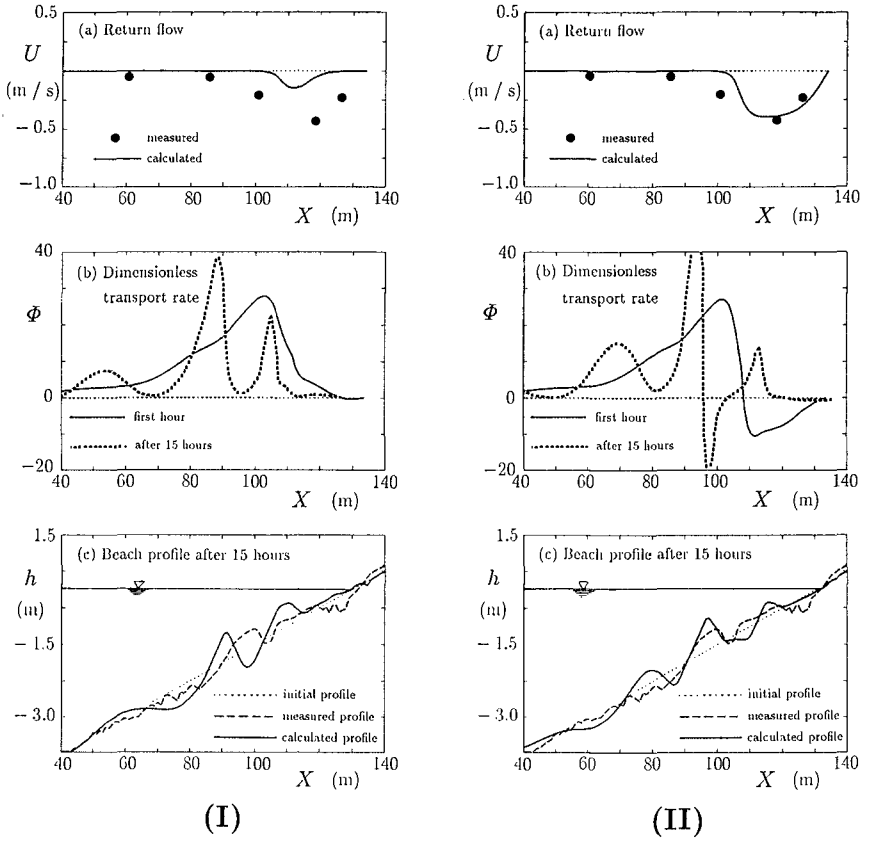

Figure 5: **Simulation results for Case 3-3 with the undertow model of (I) Sato** *et al.* **and (II) Okayasu** *et al.*.

undertow velocity of case 3-3. The performance of Okayasu *et al.*'s model in this case is better and the resulting profile is more acceptable. Strong reflection appears in the calculation of wave field for case 3-3. This reflection has much affected the transport rate distribution and consequently the profile change, specially in the offshore region. Figure 6 shows the resulting beach profile for the same case as that of Fig. 5(II) when reflected waves are removed from the wave field. A remarkable improvement is observed. In general, from the above results it is clear that the simulation of beach profile is quite sensitive to the estimation of the flow field, particularly the steady current velocity and its cross-shore gradients or distribution.

4.2 Field measurements

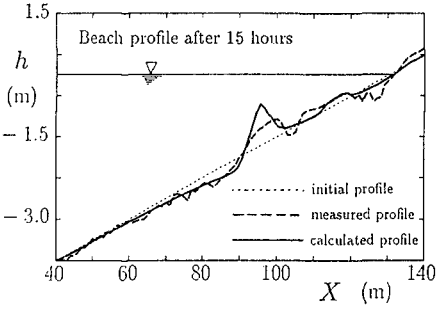

Figure 6: **Simulation results for Case 3-3 when reflection is removed (undertow model of Okayasu *et al.*).**

The model described in Sec. 3 is now applied to simulating the beach profile change which has occurred during the field measurements reported by Kuriyama (1991). Using the offshore incident wave data as the input, the wave field and its corresponding profile change are calculated every two hours.

In order to examine the sensitivity of the results on the method of estimating the undertow, at first the following equation is used for estimation of the return flow and its distribution:

$$U = -A\left(1 - \frac{E}{E'}\right)\frac{H_{1/3}^2}{D \cdot T_{1/3}} \tag{14}$$

The best agreement between the calculated and measured final profiles is obtained when $A = 5.6$ as shown in Fig. 7. It is seen that the general features of the

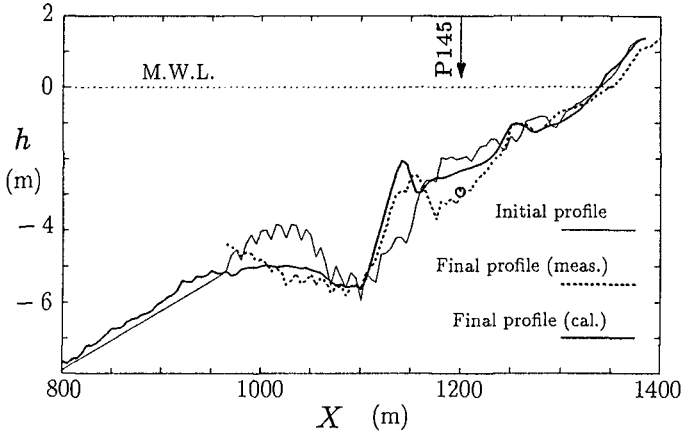

Figure 7: **Beach profile change by using Eq. (14) with $A = 5.6$.**

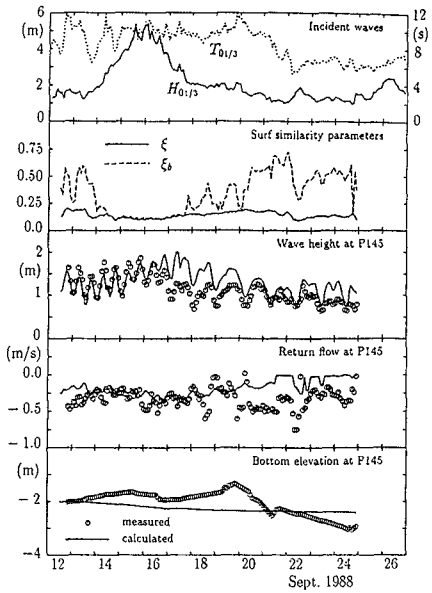

Figure 8: **Time histories of deepwater incident waves, surf similarity parameter, and wave height, undertow velocity, and bottom elevation at P145.**

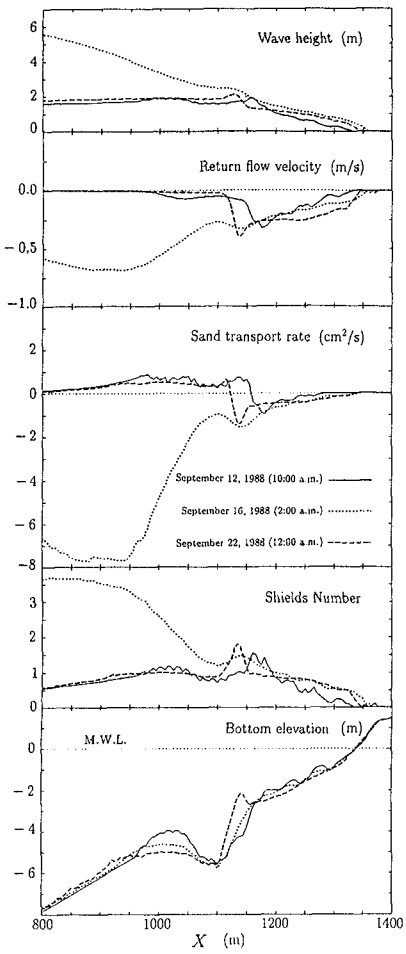

Figure 10: **Calculation results at three different times.**

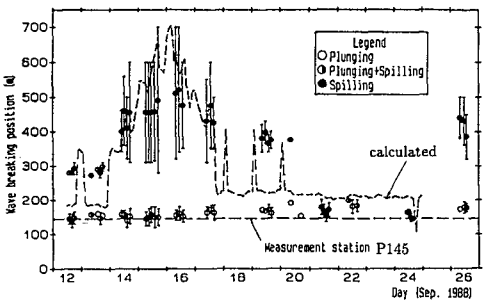

Figure 9: **Calculated and observed breaking positions.**

profile evolution, such as disappearance of the offshore bar and movement of the nearshore bar are well simulated. More details of the calculation results of this case are given in Figures 8 to 10. In Fig. 8 time variations of the deepwater incident waves and of the surf similarity parameters ξ and ξ_b are given. Also the calculated time variations of the wave height, undertow, and bottom elevation at the point P145 are plotted and compared with the measurements. The agreement between calculated and measured wave height is quite good. Estimated values of the undertow show good agreement with the measurements only during the large wave conditions when the values of ξ are nearly same as ξ_b, as was discussed in Sec. 3.3. Prediction of the bottom elevation at P145 is not satisfactory. This is attributed to the errors in estimating the cross-shore distribution of return flow, three dimensional effects, and also partly to the neglect of breaking induced turbulence. Figure 9 shows the comparison between calculated and measured breaking points. Calculated results are shown by a dashed line and are plotted on Fig. 6(2) of Kuriyama (1991). A breaking point in the calculations is defined when $\alpha'_{1/3} = \alpha_b$ which gives $P_B = 0.4$. Considering the breaking of irregular waves, this is likely to correspond to the offshore limit of the breaking zone.

In Fig. 10 some of the calculation results at three different times are given. It can be seen that values of the Shields number are usually greater than 0.5 over a large portion of the domain, indicating that sheet flow is the dominant transport mode. Large values of undertow, offshoreward transport rate, and Shields number are observed for the waves of Sept. 16, 1988. It is around this time that the offshore bar disappears and it is well simulated by the model. The large waves on the other hand, have less effect on the nearshore profile, and the change in the nearshore region is mainly occurred after the storm is finished.

As for the next case, Equation (6) is used for calculating the undertow. Figure 11 shows the time variation of the undertow velocity and its comparison with the measurements at the point P145. In Fig. 12 the result of profile simulation

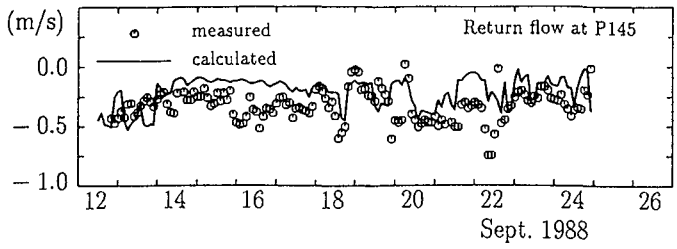

Figure 11: **Undertow velocity at the point P145 using Eq. (6).**

is given. Although an improvement in the estimation of the undertow velocity is observed, but the resulting beach profile does not show an improvement. The reason is attributed to the errors in estimation of cross-shore distribution of the undertow, determination of the bottom slope at the breaking point, effect of alongshore variation in the flow field and the existence of rip currents, and the

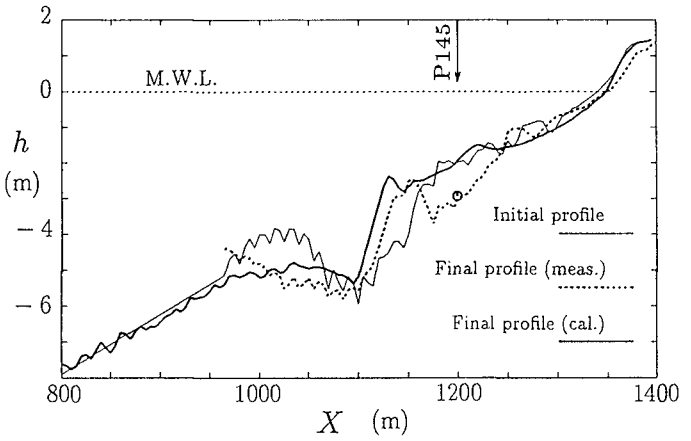

Figure 12: **Beach profile change by using Eq. (6).**

neglect of breaking induced turbulence. Further study on modelling of the flow field is thus required for more improvements.

5. Conclusions

A new and detailed model of beach profile change is presented. It incorporates, explicitly, the asymmetry of the near-bottom orbital velocity and the undertow, into the transport of bottom sediment. The model is examined by using the data of beach profile change obtained from prototype scale laboratory experiments as well as field measurements. It is shown that quite accurate profile simulation is possible when the details of the flow field and transport mechanism are considered.

The results show strong dependency on the distribution and magnitude of the undertow velocity. For further improvements, accurate and general models for estimation of the near-bottom orbital velocity profile in the surf zone and for undertow velocity are required. The so-called swash transport is not included in the present model and therefore the profile change around the shoreline is not well simulated. Modelling of the swash zone is left for a future study.

References

Dibajnia, M., and A. Watanabe 1992: Sheet flow under nonlinear waves and currents, *Proc. 23rd Int. Coastal Eng. Conf., ASCE*, pp. 2015-2028.

Dibajnia, M., T. Shimizu, and A. Watanabe 1992: Profile change of a sheet flow dominated beach, *Proc. 39th Japanese Annual Conf. on Coastal Eng., JSCE*, pp. 301-305 (in Japanese).

Isobe, M., 1987: A parabolic equation model for transformation of irregular

waves due to refraction, diffraction and breaking, *Coastal Eng. in Japan*, Vol. 30, No. 1, pp. 33-47.

Isobe, M., and K. Horikawa 1981: Change in velocity field in and near the surf zone, *Proc. 28th Japanese Annual Conf. on Coastal Eng., JSCE*, pp. 5-9 (in Japanese).

Kajima, R., T. Shimizu, K. Maruyama, and S. Saito 1982: Experiments on beach profile change with a large wave flume, *Proc. 18th Int. Coastal Eng. Conf., ASCE*, pp. 1385-1404.

Okayasu, A., A. Watanabe, and M. Isobe 1990: Modeling of energy transfer and undertow in the surf zone, *Proc. 22nd Int. Coastal Eng. Conf., ASCE*, pp. 123-135.

Sato, S., M. Fukuhama, K. Horikawa 1988: Measurements of near-bottom velocities in random waves on a constant slope, *Coastal Eng. in Japan*, Vol. 31, No. 2, pp. 219-228.

Suzuki, k., A. Watanabe, M. Isobe, and M. Dibajnia 1994: Experimental study on transport of sediment with mixed-grain size due to oscillatory flow, *Proc. 41st Japanese Annual Conf. on Coastal Eng., JSCE*, pp. 356-360 (in Japanese).

Watanabe, A., and M. Dibajnia 1988: A numerical model of wave deformation in surf zone, *Proc. 21rd Int. Coastal Eng. Conf., ASCE*, pp. 578-587.

Watanabe, A., T. Hara, and K. Horikawa 1984: Study on breaking condition for compound wave trains, *Coastal Engineering in Japan, JSCE*, Vol. 27, pp. 71-82.